AUT Journal of Mechanical Engineering

AUT J. Mech. Eng., 8(1) (2024) 67-82
DOI: 10.22060/ajme.2024.22847.6080

Experimental and Image Processing Study on the Effect of the Cavitation Phenomenon in a Nozzle Injector on the Hydrodynamic Behavior of the Spray

Saeid Azizi, Mohammad Taghi Shervani-Tabar *

Department of Mechanical Engineering, University of Tabriz, Tabriz, Iran

ABSTRACT: The hydrodynamic behavior of liquid spray is influenced by the geometry of the injector nozzle, which has a significant impact on the combustion process and quality of fuel atomization. In this survey, transparent and visible nozzles were fabricated from Plexiglas to facilitate experimental visualization of the nozzle interior and enhance the accuracy of liquid spray investigation. To achieve this, three types of nozzles with varying orifice coefficients were prepared. Results showed that at a certain pressure, for a divergent conical nozzle, the intensity of cavitation increases, and it's very prone to cavitation. Conversely, the convergent conical nozzle suppresses cavitation. As the pressure of fluid injection rises within nozzles, cavitation bubbles persist until reaching the orifice's end, resulting in the super-cavitation phenomenon. Further, increasing injection pressure triggers the hydraulic flip phenomenon. The occurrence of the super-cavitation phenomenon causes uniform droplet distribution of the resulting spray. In other words, The pressure corresponding to the occurrence of the super-cavitation phenomenon has a better droplet breakup and distribution (divergent conical nozzle with an injection pressure of 3 MPa). At a certain injection pressure with decreasing k factor outlet volume flow rate of the nozzle decreases and the spray cone angle increases. Therefore, the desired macroscopic characteristic of the spray could be determined by specifying the k factor.

Review History:

Received: Dec. 15, 2023
Revised: May, 12, 2024
Accepted: Jul. 05, 2024
Available Online: Jul. 23, 2024

Keywords:

Visualization Experiment
Cavitation
Nozzle Injector
Spray

1- Introduction

Many light and heavy vehicles in the transportation and agricultural industries depend on diesel engines, and the largest vessels use diesel engines. In recent years, these engines have faced limitations that need to increase the quality of fuel combustion and produce less emission[1, 2]. Diesel engine engineers seek to improve the combustion quality of the fuel and the combustion process by providing a variety of fuel injection systems and the use of alternative fuels[3, 4].

Since the quality of atomization and fuel spray specifications control fuel-air mixing and the intensity of local mixing in the mixing chamber, the performance of diesel engines and pollutant emissions depends on the fuel spray and fuel atomization specifications[5, 6]. The spray characteristics include spray tip penetration (STP), droplet size distribution, and spray cone angle are influenced by nozzle geometry. This might be due to the cavitation and turbulent flow inside the nozzle[7, 8]. In diesel injector nozzles, the cavitation and turbulent flow have a decisive influence on the atomization of the fuel spray [9, 10]. For the comprehension of the spray atomization mechanism, it is necessary to clarify the characteristics of the cavitation flow. In recent years, numerous numerical researches have been performed to scrutinize the probable impacts of the nozzle injector geometry on the nozzle internal flow and fuel spray characteristics[11-13]. In the meantime, experimental studies have been conducted from time to time[14-16]. Sun et al.[17] numerically studied the influence of the coefficient of the orifice on the internal flow of the nozzle injector and the specification of cavitation. Results indicated that with increasing orifice coefficient, the flow coefficient, and mass flow rate substantially grow also, and the mean vapor volume fraction decreases with the increase of the orifice coefficient. They noted that cavitation bubbles reduced as they used orifices with a higher factor. The stifle of cavitation bobbles is stronger for the conical orifice in comparison with the inverted conical orifice. Tang et al.[5] a comprehensive study that investigated the effect of the conicity of the nozzle orifice on spray macroscopic properties at high injection pressure. The results illustrated improving the flow coefficient of the orifice slightly increases the spray tip penetration. They pointed out that in conical nozzles, because of the reduction of flow turbulence and cavitation inside the nozzle, the raised exit flow velocity and the debilitated initial breakup cause a slight increase in spray penetration. However, the effect of the orifice coefficient is not as much as injection pressure and ambient pressure[18, 19]. Dai et al.[20] studied the influence of curved nozzle structures on cavitation characteristics in

*Corresponding author's email: msherv@tabrizu.ac.ir

high-pressure common rail diesel engines. Results indicate that curved nozzles effectively reduce cavitation levels, with greater curvature correlating to decreased cavitation. Shervani-Tabar et al.[21] studied the effect of R/D (ratio of the curvature radius of orifice inlet to orifice Diameter) on the spray characteristics as one of the main reasons for the generation of cavitation bubbles in the orifice of nozzle injector. The results showed that with increasing of R/D, the values of SMD increase and resulting in a decline in cavitation significantly. Finally, it leads to a lower quality of atomization. They also illustrated that the largest spray tip penetration occurs at R/D=0 which is coincident with the occurrence of the strongest cavitation inside the nozzle. Moreover, with an increase of R/D, spray tip penetration reduces, and this is accompanied by cavitation suppression. Jalili et al.[22] conducted a numerical investigation into the influence of nozzle geometry on spray trajectory and breakup. Their results revealed distinct spray trajectories for elliptic and circular nozzles. With escalating turbulence, vortices in the flow accumulated greater energy, resulting in heightened vorticity. This, in turn, caused the spray breakup to occur nearer to the injector output, attributable to shifts in the breakup mechanism.

The importance of the flow behavior inside the injector nozzle and its effect on the spray characteristics induced researchers to design visible nozzles in real size or scaled up to observe the phenomenon of cavitation and flow inside the nozzle injector[23-25]. Ghiji et al.[26] studied diesel engine spray dynamics near the nozzle exit. they reported that cavitation development leads to liquid detachment from nozzle walls, reducing boundary layer effects, in-nozzle turbulence, and increasing liquid jet velocity. Zhixia et al.[24, 27] tested a transparent nozzle to scrutinize the effect of needle lift inside the nozzle injector on cavitation growth and the appearance of string cavitation. They reported that the growth of cavitation bubbles is affected by the injection pressure, and higher injection pressures lead to earlier cavitation. According to their results, the appearance of string cavitation, which increases the spray cone angle, depends on three factors, including injection pressure, needle lift, and the shape of the nozzle sac. Ding et al.[28] investigated how injection pressure and fuel properties affect near-nozzle spray patterns at the start of the fuel spray. They showed a direct correlation between mushroom length and fuel viscosity, where higher viscosity resulted in a longer mushroom length. Initially, the mushroom traveled faster than the trail region, contributing to the lengthening of the mushroom. A review of previously published articles shows that there have not been enough studies about the effect of the conicity of the orifice on the generation of cavitation and flow behavior inside a transparent injector nozzle. In the present work, the image processing capability was employed to analyze images of nozzle internal flow and spray.

This verification provides a better understanding of the flow behavior inside the injector nozzle and its effect on the fuel spray characteristics. The occurrence of the cavitation phenomenon inside the scaled-up injector nozzle was observed by employing a visible transparent nozzle. Three similar nozzles with varying conicity were utilized to investigate the influence of orifice geometry on both cavitation phenomenon and turbulence within the injector nozzle. Then, the effects of the flow behavior inside the injector nozzle on the macroscopic characteristics of the spray were evaluated[29].

2- Experimental equipment and methodology

The primary aim of this research is to evaluate the feasibility of observing and imaging the internal flow within the injector nozzle and the resulting spray. An experimental apparatus was constructed and utilized for this purpose. Fig. 1 shows a schematic of the experimental device, In which the fluid is sprayed into the atmosphere through transparent nozzles at injection pressures ranging from 1 to 4 MPa. The spray is collected by a chamber and then returned to the cycle by the pump. Three transparent nozzles with different conical degrees of the orifice were used to investigate how injector nozzle geometry and orifice conical degree affect the internal flow within the injector nozzle. This probe aimed to understand their influence on the hydrodynamic behavior of the fluid spray. Each nozzle's internal flow and fluid spray were captured using a camera set at a distance of 1 meter, with an image resolution of 4288 * 2856 pixels. Finally, the images were transferred to a computer for image processing. In the results section, both real and processed images are provided. A pressure gauge with an accuracy of 0.1 bar was used for the measurements. Each test was conducted five times at different pressures to ensure accuracy and eliminate potential errors.

2- 1- Nozzle

One of the main objectives of this study is to observe and record the internal flow of the injector nozzle. For this purpose, transparent nozzles made of Plexiglas with imaging capability have been designed and produced. Plexiglas, due to its high transparency and low light refraction, allows having high-quality images. In the present work, scaled-up nozzles, approximately 10 times larger than the size of real nozzles are used. Three types of nozzles with the titles of convergent conical (k =0.25), divergent conical (k =-0.25), and cylindrical nozzles (k= 0) have been used. All nozzles have the same orifice outlet cross-section and are equal to 1.5× 1 mm^2, and their orifice length is equal to 10 mm. The conical degree of the orifice for the cylindrical, divergent conical, and convergent conical nozzles are considered zero, +8, and -8, respectively.

2- 2- Verification

In Fig. 3 the flow behavior inside the orifice of the cylindrical injector nozzle for different injection pressures of 1, 2, 3, and 4 MPa have been compared with work of the Akira et al.[30]. Comparison of the flow patterns generation inside the nozzle orifice of both works displays; that there is a reasonable agreement between the results. Cavitation bubbles are observed to initiate, develop, and persist throughout the entirety of the nozzle orifice in both studies.

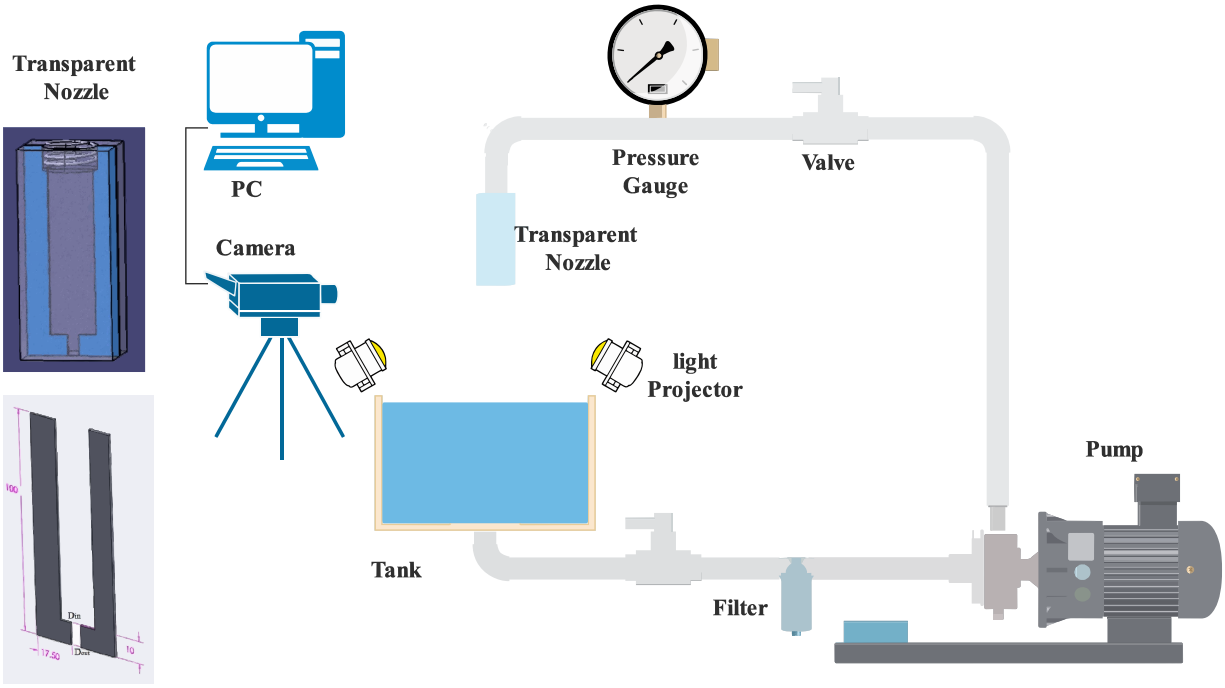

Fig. 1. Schematic of the experimental setup.

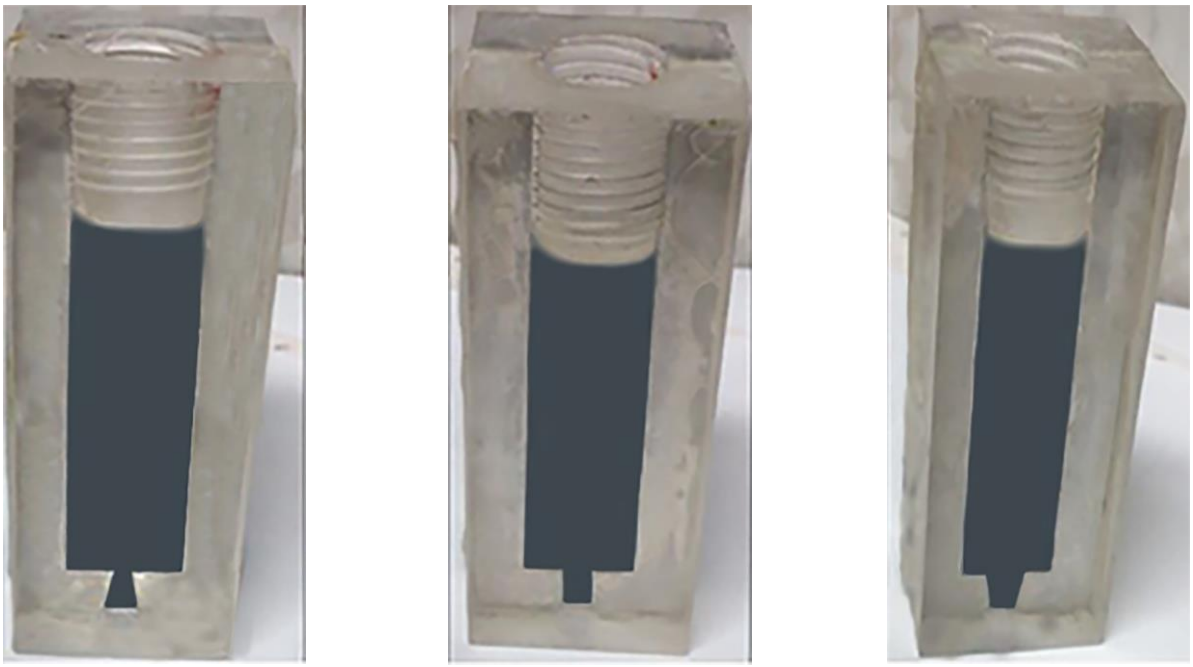

Fig. 2. Real transparent nozzles: a) divergent conical nozzle; b) cylindrical nozzle c) convergent conical nozzle.

Table 1. Geometric dimensions of the tested nozzles

Geometric characteristics	Divergent conical nozzle	Cylindrical nozzle	Convergent conical nozzle
$D_{in}(mm)$	2.48	5	7.52
$D_{out}(mm)$	5	5	5
$K=(D_{in} - D_{out}) /10$	-0.25	0	0.25
$L(mm)$	10	10	10
$W(mm)$	1.50	1.50	1.50

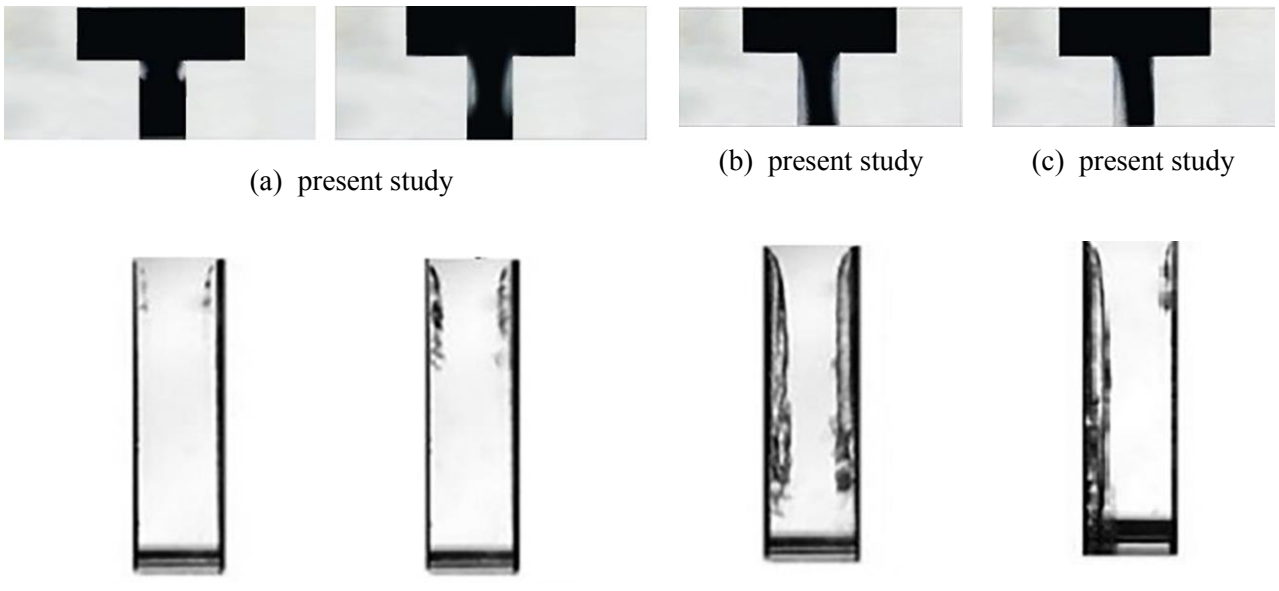

(a) present study (b) present study (c) present study

(d) Akira et al (e) Akira et al (f) Akira et al

Fig. 3. Comparision iternal flow of cylindrical nozzle studied in the present work with results of Akira et al. [30]. a,d) developing cavitation b,e) super-cavitation c,f) hydraulic flip.

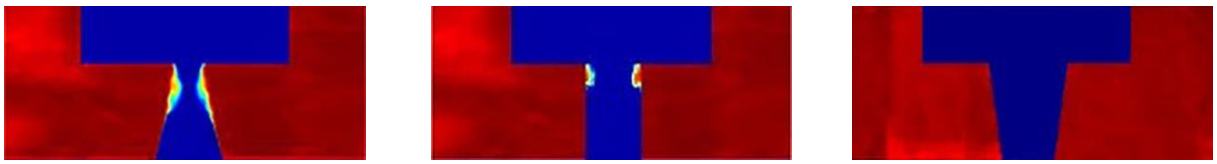

(a) (b) (c)

Fig. 4. Flow inside the different nozzles at p_{inj}=1 MP; a) divergent conical nozzle, b) cylindrical nozzle, and c) convergent conical nozzle

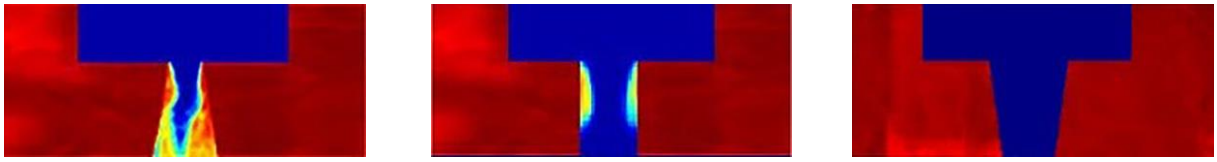

(a) (b) (c)

Fig. 5. Flow inside the different nozzles at pinj=2 MP; a) divergent conical nozzle, b) cylindrical nozzle, and c) convergent conical nozzle

2- 3- Image processing

Digital images are produced by a camera and then transmitted to an image processing system. In image processing, a digital image is defined as a function F(x, y) in which x and y are the spatial coordinates of each point, and the value of (F) is the image intensity at that point. Adjusting image intensity is one of the steps in image processing that has been used to improve image quality and brightness. To process the image, In RGB (Red, Green, Blue) images, each pixel is represented by three intensity values corresponding to the amount of red, green, and blue light. Each of these values ranges from 0 to 255. Then, in the process, the image noises are removed from the image, which can be extra light and objects around the desirable image. Separation of the desired image from the image background is one of the most important steps in image processing, which is done using the edge detection method and based on determining a certain threshold.

The histogram serves as a vital tool in image processing, allowing for the identification of the dispersion and arrangement of spray particles. It represents the frequency of pixel intensities in the red, green, and blue channels of an RGB image separately. Essentially, it depicts the number of occurrences of each pixel intensity level through a graphical representation. In darker images, the RGB values (or histogram) tend to concentrate in the lower range near zero, whereas in lighter images, they are more concentrated in the higher range closer to 255. In a well-distributed and atomized spray, the histogram spans across the entire 0 to 255 range for each color channel. Conversely, poorly atomized sprays exhibit dense and scattered areas within the image histogram.

3- Results and discussion

3- 1- Effect of nozzle geometry on internal flow

Fig. 4 shows the fluid flow inside the divergent, cylindrical, and convergent conical nozzles at an injection pressure of 1 MPa. Very tiny cavitation bubbles can be seen at the inlet edges of divergent conical and cylindrical nozzles, indicating the inception of the cavitation in these nozzles. The bulk of cavitation bubbles developed in the divergent conical nozzle is slightly more than that of the cylindrical nozzle while, no cavitation bubbles inside the convergent conical nozzle. Fig. 5 shows the flow inside the nozzle of the injectors at the injection pressure of 2 MPa. Examination of the flow inside the divergent conical nozzle shows that the bulk of the cavitation bubbles increased rapidly compared to

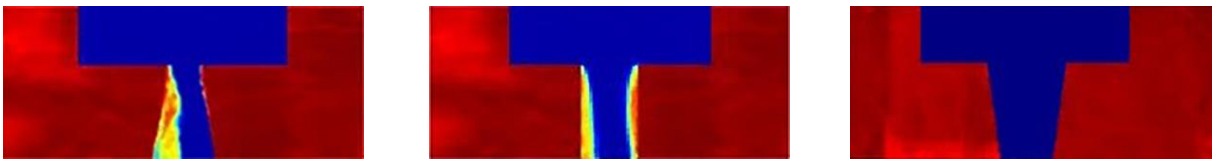

(a) (b) (c)

Fig. 6. Flow inside the different nozzles at p_{inj}=3 MP; a) divergent conical nozzle, b) cylindrical nozzle, and c) convergent conical nozzle

the 1 MPa pressure and extended to the orifice outlet. In a cylindrical nozzle at the injection pressure of 2 MPa, the cavitation bubbles have grown significantly compared to the pressure of 1 MPa and have continued almost to the middle of the orifice length. The bulk of cavitation bubbles in the cylindrical nozzle is relatively smaller than in the divergent conical nozzle, so it is expected that the flow inside the divergent conical nozzle is more severely disturbed than in a cylindrical nozzle, and the possible effects of these disturbances on the nozzle output characteristics will be observed. The convergent conical nozzle flow at a pressure of 2 MPa had no significant response to the increase of injection pressure of 1 MPa in terms of turbulence and the generation of the cavitation bubble. The processed images of the flow of the injector nozzle at the injection pressure of 3 MPa show, that in the divergent conical nozzle, the cavitation bubbles are formed only on one side of the orifice wall and continue to the orifice outlet Fig 6. In other words, for the divergent conical nozzle, the hydraulic flip phenomenon events at the pressure of 3 MPa Fig. 6(a). In the case of the cylindrical nozzle, with increasing injection pressure up to 3 MPa, the bulk of the cavitation bubbles increases, and the cavitation bubbles on both sides of the orifice wall reach the orifice output end. In fact, for cylindrical nozzles, the super-cavitation phenomenon occurred at a pressure of 3 MPa, while in a divergent conical nozzle, this phenomenon occurred at a pressure of 2 MPa Fig. 6(b). This fact is because the sudden change in the cross-section area of the orifice in the divergent conical nozzles is greater than in the cylindrical nozzles, and this causes a greater local pressure drop in the inlet area of the divergent conical nozzle than in cylindrical nozzles and provides better cavitation within the injector nozzle orifice. For the injection pressure of 3 MPa, the flow conditions inside the convergent conical nozzle have not changed from the former state Fig. 6(c). In fact, in convergent nozzles, due to the slight decrease in the cross-section area of the orifice to the divergent conical and cylindrical nozzles, the local pressure has not decreased so much that it leads to the formation of cavitation bubbles. In other words, the sharp edge of the nozzle orifice, which is one of the main causes of the cavitation inside the nozzle orifice, is much less in the convergent nozzle compared to cylindrical and divergent nozzles, so this fact causes the convergent nozzle to have a smaller cavitation region than divergent conical and cylindrical nozzles.

3- 2- Effect of nozzle geometry on fluid spray

Fig. 7 shows the sprays of divergent conical, cylindrical, and convergent conical injector nozzles at different fluid injection pressures of 1-3 MPa. In the processed images of the spray, a blue-red color spectrum is used, where blue represents low spray density and red represents high spray density. It is evident that the spray from the divergent conical nozzle spreads widely in the atmosphere compared to the other two sprays, Fig 7. a. The obtuse angle of the orifice walls in divergent nozzles directs the fluid away from the center, leading to greater spray spread. In divergent conical nozzle sprays, the density is higher near the nozzle outlet and gradually decreases towards the end, indicating improved spray droplet atomization. The intensity of spray density is higher in the central areas than at the edges, resulting in larger droplets at the center. For cylindrical nozzle spray (Fig. 7b), the injection pressure is not sufficient for wide spraying. The spray density is relatively uniform during spraying, with less density at the edges compared to the center. In Fig. 7c, the convergent nozzle spray is thinner and has a weaker spray droplet distribution compared to the other nozzles. The density is highest in the central areas, with a slight reduction near the nozzle outlet due to the fluid being directed towards the center by the orifice walls.

The divergent conical nozzle spray at the injection pressure of 2 MPa has been shown in Fig. 7d. It appears that the bulk of the spray has increased compared with 1 MPa, and the density of fluid droplets has grown during the spray. In Fig. 7e, The outlet sprays from the cylindrical nozzle at a

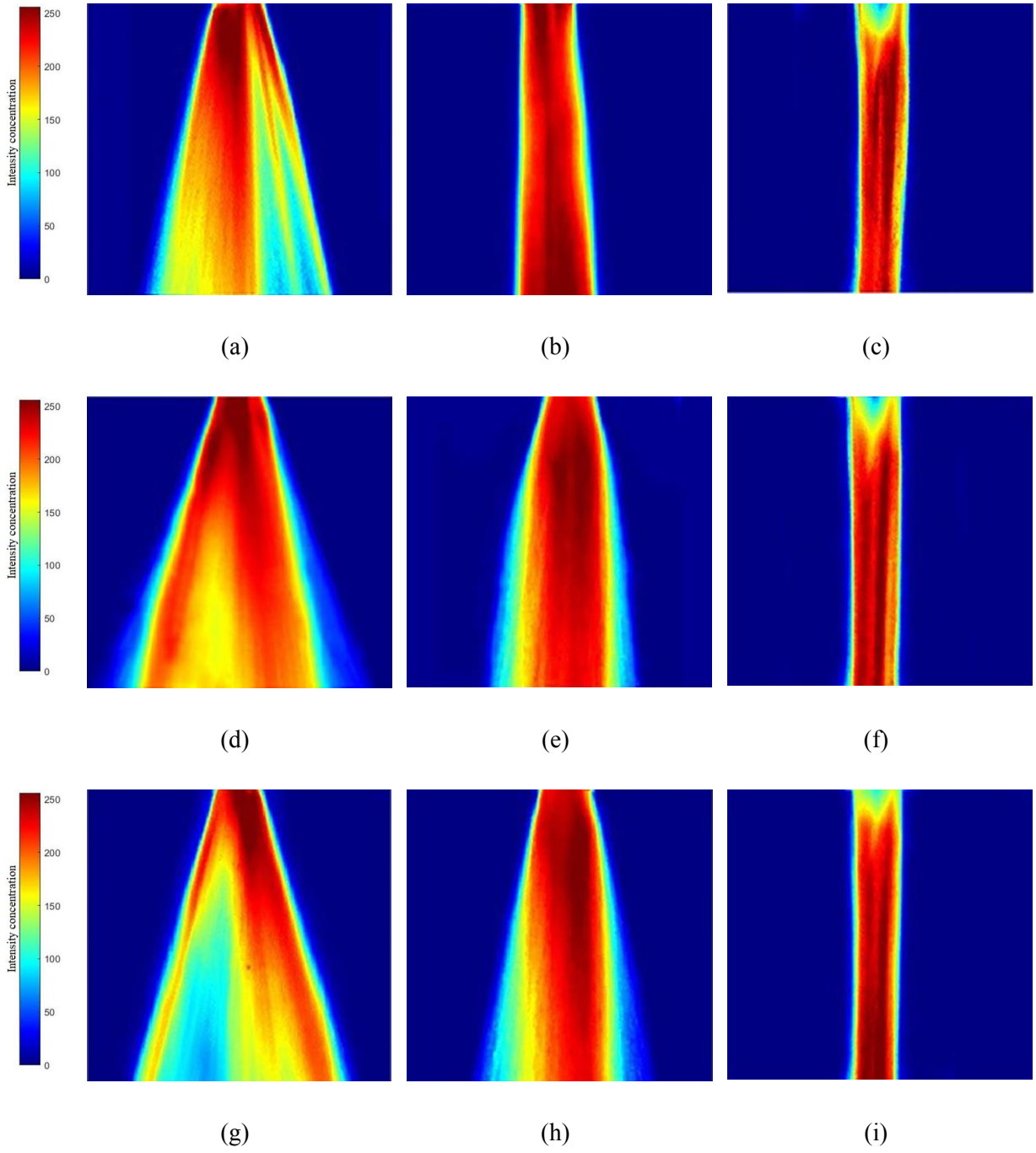

Fig. 7. The processed images of the liquid spray of different nozzles at different injection pressures. a) divergent conical nozzle with p_{inj}=1 MPa, b) cylindrical nozzle with p_{inj}=1 MPa, c) convergent conical nozzle with p_{inj}=1 MPa, d) divergent conical nozzle with p_{inj}=2 MPa, e) cylindrical nozzle with p_{inj}=2 MPa, f) convergent conical nozzle with p_{inj}=2 MPa, g) divergent conical nozzle with p_{inj}=3 MPa, h) cylindrical nozzle with p_{inj}=3 MPa, i) convergent conical nozzle with p_{inj}=3 MPa.

pressure of 2 MPa show more distribution than at a pressure of 1 MPa. Fig. 7f displays the convergent nozzle spray at an injection pressure of 3 MPa.

In Fig. 7g, it is clear that the divergent nozzle spray has a lower density at the injection pressure of 3 MPa than at the pressure of 2 MPa. The effect of the occurrence of the hydraulic flip phenomenon inside the injector nozzle at this pressure is seen as a decrease in the intensity of the spray density on one side of the spray plume so that it can be expected that the output volume flow rate would also decrease slightly. Nozzle turbulent flow originated from the hydraulic flip leads to uneven spray distribution. Fig. 7h shows the spray of the cylindrical nozzle at an injection pressure of 3 MPa has scattered widely and is distributed better than at lower injection pressures. The occurrence of the super-cavitation phenomenon in the nozzle had a positive effect on the spray distribution as both the primary and secondary breakup of the droplets increased compared to the 2 MPa injection pressure. Fig.7i relates to the convergent conical nozzle at an injection pressure of 3 MPa. As the injection pressure increases, there is a discernible trend whereby the bulk of the spray plumes narrows in comparison to lower injection pressures. This behavior of the spray is attributed to the nozzle's geometry.

As evident from the histogram of the spray in Fig. 8a, there is a notable congestion of spray intensities within the range of 100-200, indicating a significant occurrence of breakup after exiting the divergent nozzle. This concentration of intensities suggests that a large portion of the spray experienced fragmentation or break up into smaller droplets as it traveled through the divergent nozzle. The increased frequency of intensities within this range implies a more dispersed distribution of droplet sizes, potentially resulting in improved atomization and dispersion characteristics within the spray plume. Conversely, in the case of the cylindrical nozzle spray depicted in Fig. 8b, the histogram shifts towards the right, with an increased pixel intensity around 250. This shift indicates a higher concentration of larger droplets or a lower occurrence of breakup events compared to the divergent nozzle. The distribution skewed towards higher intensity values suggests that a larger proportion of droplets remained relatively intact or experienced minimal fragmentation during their passage through the cylindrical nozzle. This phenomenon may be attributed to the narrower exit geometry of the cylindrical nozzle, which imposes less disruption on the flow and droplet breakup process compared to the divergent nozzle. Moreover, the histogram for the convergent nozzle spray (Fig. 8c) exhibits a higher frequency of zero intensity, indicating a more distributed spray pattern and a smaller diffusion angle compared to the other two nozzles. The predominance of zero intensity values suggests that a significant portion of the spray is composed of smaller droplets or mist, resulting in a more diffuse and tightly concentrated spray pattern. This distribution characteristic is consistent with the convergent geometry of the nozzle, which accelerates and compresses the flow, leading to enhanced atomization and spray dispersion. Overall, the histograms provide valuable insights into the breakup behavior and spray distribution characteristics of different nozzle designs, highlighting the influence of nozzle geometry on spray formation and dispersion.

It can be seen, in the histogram of spray in Fig. 8d, that the congestion of intensity is high in the range between 150-220; this proves that the primary breakup of droplets has increased, and the frequency of intensity lower than 150 which indicate the second breakup have decreased. The occurrence of super-cavitation in the nozzle fosters primary breakup at the near nozzle and, it is expected that the second breakup grows as the spray continues. Although, it is not seen at this spray length. Comparing histograms of injection pressures of 1 MPa and 2 MPa for cylindrical nozzle shows that, almost all around of spray plume, the nozzle with higher pressure has higher intensity values related to lower one (Fig. 8e) . In Figure 8f, the frequency of intensity between 0-250 for the convergent conical nozzle is lower than that for both the divergent and cylindrical nozzles. This indicates a reduction in the spray distribution under these specific conditions.

As can be seen in Fig. 8g, almost all ranges of Hue intensity have higher values of frequency of intensity, which means that a wider surface has drops of spray and results in better distribution of fluid. Fig. 8h illustrates the histogram of cylindrical nozzle spray at a pressure of 3 MPa. The distribution of the histogram in this nozzle shows a more uniform pattern than the divergent nozzle. This is due to the conical shape of the orifice that causes scattering of the fluid, where the intensity concentration is high in the range between 100-220. In Fig. 8i, the histogram analysis of the convergent nozzle spray at a pressure of 3 MPa indicates that despite the increase in fluid injection pressure, there is minimal change in the frequency of zero intensity compared to the previous case. This suggests that the spray cone angle remains very low in this nozzle configuration, potentially leading to inadequate spray droplet distribution. The similarity in histograms between the current and previous cases implies a consistent spray pattern, indicating that further adjustments may be necessary to achieve optimal spray characteristics in this nozzle design.

3- 3- Effect of injection pressure on inside flow and spray

In this section, the effect of injection pressure on nozzle internal flow and spray was studied. The cylindrical nozzle was employed at various injection pressures ranging from 1-4 MPa. Patterns of cavitation occurrence inside the transparent injector nozzle and its effects on the macroscopic characteristics of the spray were recorded. Fig. 9 shows the internal flow of the cylindrical nozzle and outlet spray. The commencement of turbulent flow began with the slight appearance of cavitation bubbles in the inlet of the nozzle orifice at an injection pressure of 1 MPa. In this state, the spray cone angle was 16.44 degrees. With increasing pressure to 2 MPa, the inside flow reaction was increased with the increase in bubble bulk, and it continued to the middle of the orifice on both sides of the orifice walls. In this condition, the spray cone angle soared to 27.93 degrees. At an injection pressure of 3 MPa, cavitation bubbles were developed at the end of the orifice. The effect of this phenomenon was

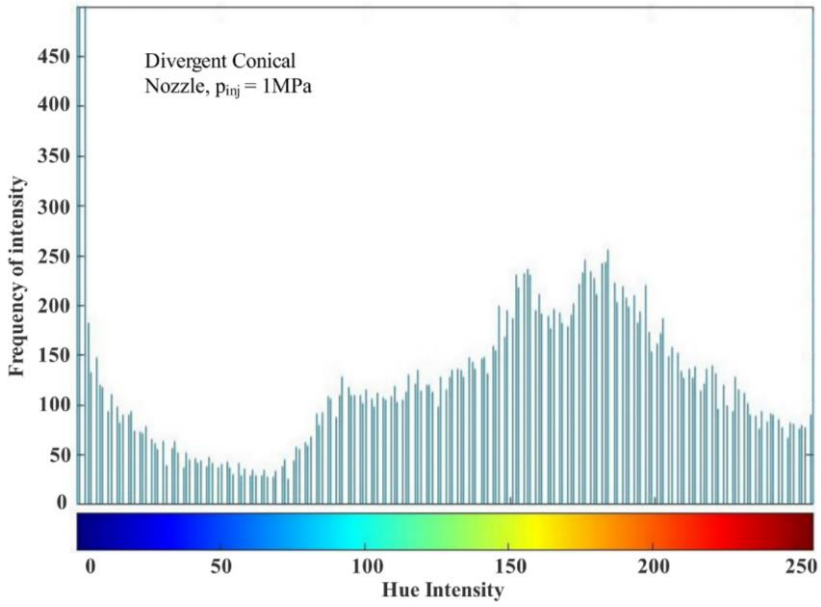

(a)

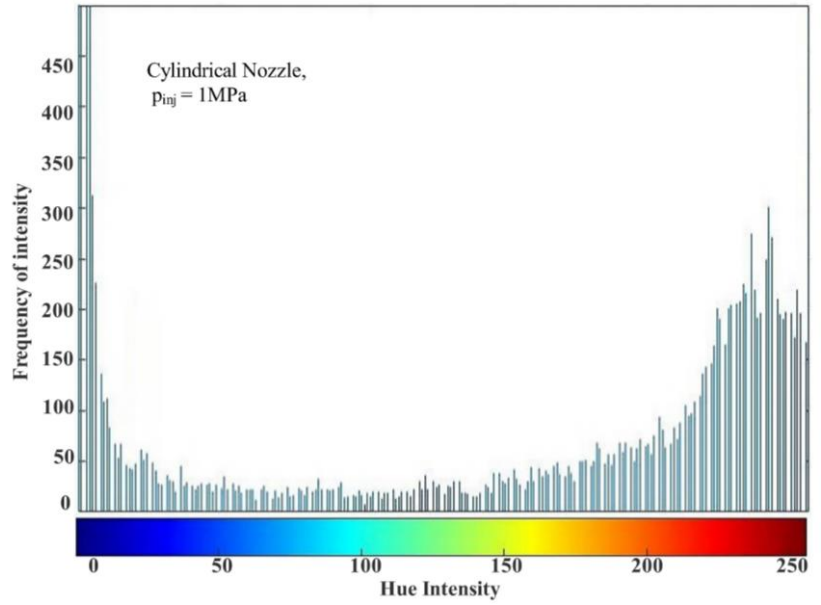

(b)

Fig. 8. The histogram of different nozzle sprays at different injection pressures; a) divergent conical nozzle with p_{inj}=1 MPa, b) cylindrical nozzle with p_{inj}=1 MPa, c) convergent conical nozzle with p_{inj}=1 MPa, d) divergent conical nozzle with p_{inj}=2 MPa, e) cylindrical nozzle with p_{inj}=2 MPa, f) convergent conical nozzle with p_{inj}=2 MPa, g) divergent conical nozzle with p_{inj}=3 MPa, h) cylindrical nozzle with p_{inj}=3 MPa, i) convergent conical nozzle with p_{inj}=3 MPa. (Colntinued)

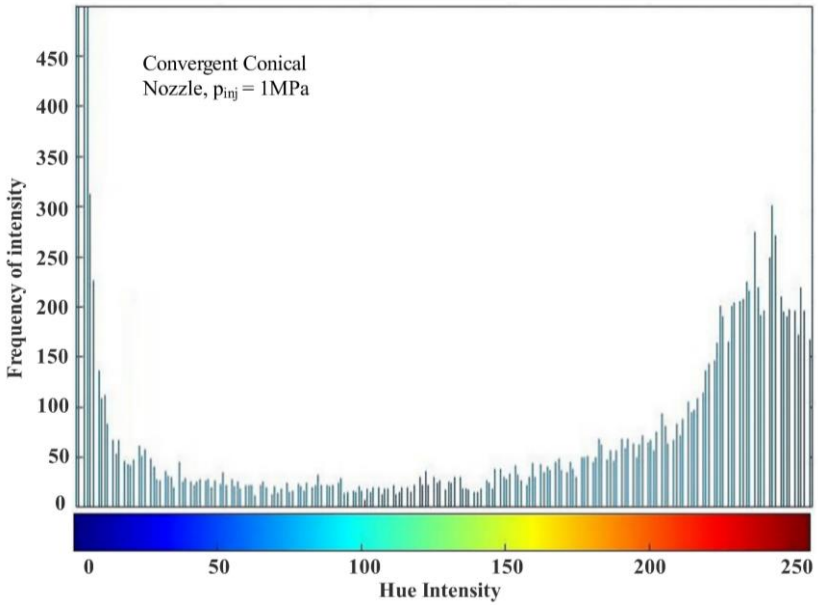

(c)

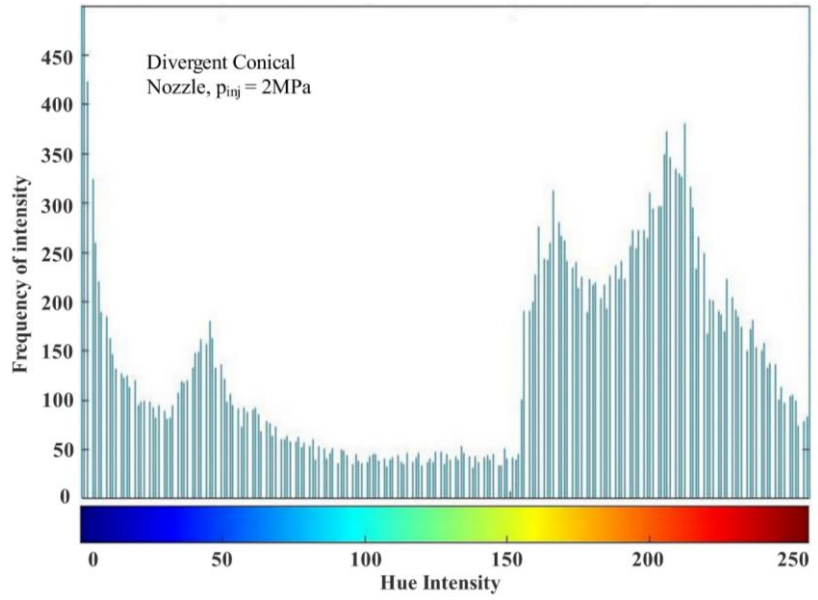

(d)

Fig. 8. The histogram of different nozzle sprays at different injection pressures; a) divergent conical nozzle with p_{inj}=1 MPa, b) cylindrical nozzle with p_{inj}=1 MPa, c) convergent conical nozzle with p_{inj}=1 MPa, d) divergent conical nozzle with p_{inj}=2 MPa, e) cylindrical nozzle with p_{inj}=2 MPa, f) convergent conical nozzle with p_{inj}=2 MPa, g) divergent conical nozzle with p_{inj}=3 MPa, h) cylindrical nozzle with p_{inj}=3 MPa, i) convergent conical nozzle with p_{inj}=3 MPa. (Colntinued)

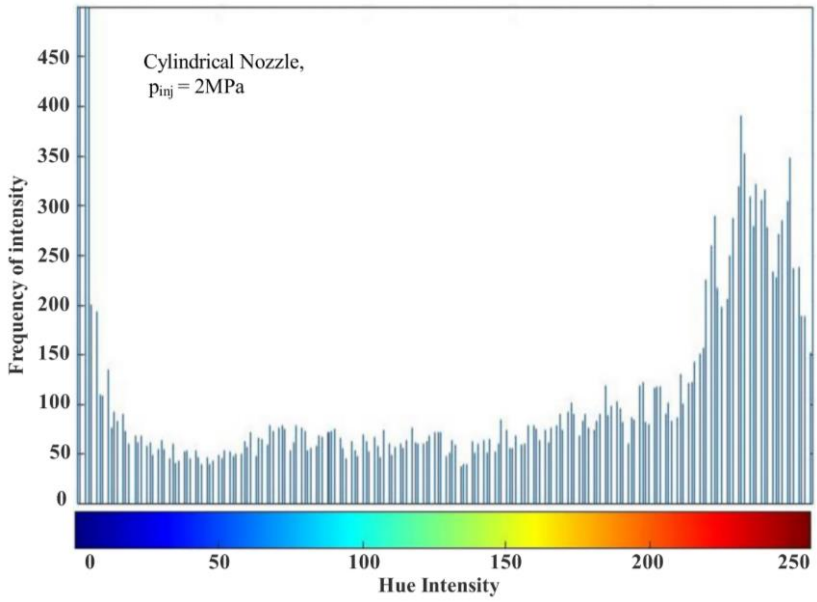

(e)

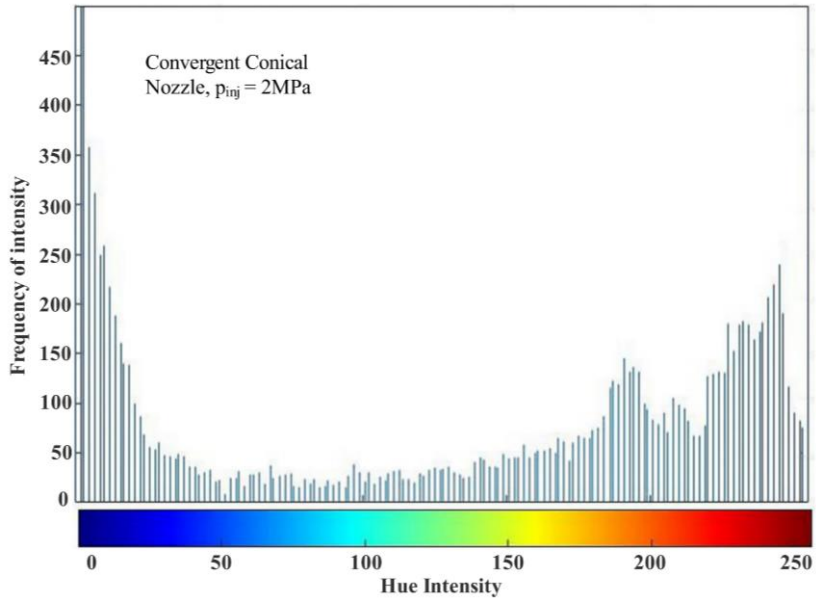

(f)

Fig. 8. The histogram of different nozzle sprays at different injection pressures; a) divergent conical nozzle with p_{inj}=1 MPa, b) cylindrical nozzle with p_{inj}=1 MPa, c) convergent conical nozzle with p_{inj}=1 MPa, d) divergent conical nozzle with p_{inj}=2 MPa, e) cylindrical nozzle with p_{inj}=2 MPa, f) convergent conical nozzle with p_{inj}=2 MPa, g) divergent conical nozzle with p_{inj}=3 MPa, h) cylindrical nozzle with p_{inj}=3 MPa, i) convergent conical nozzle with p_{inj}=3 MPa. (Colntinued)

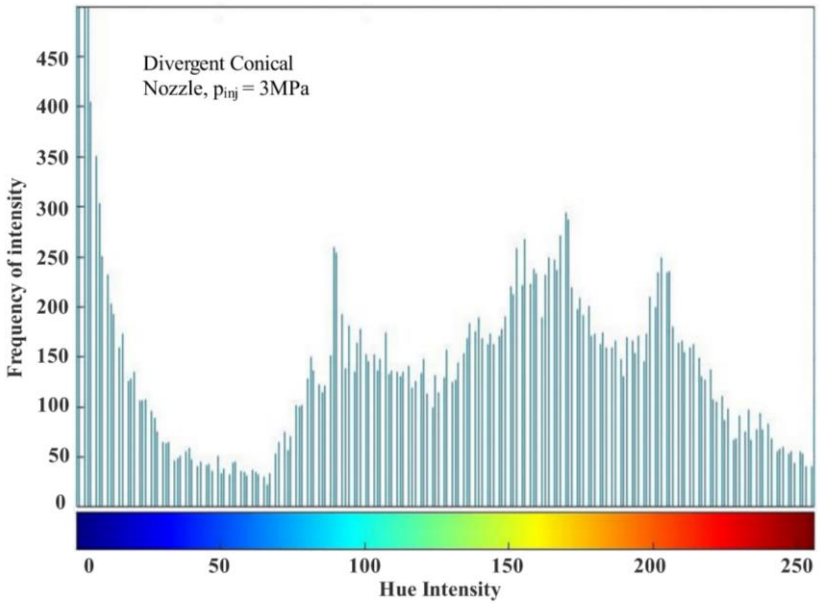

(g)

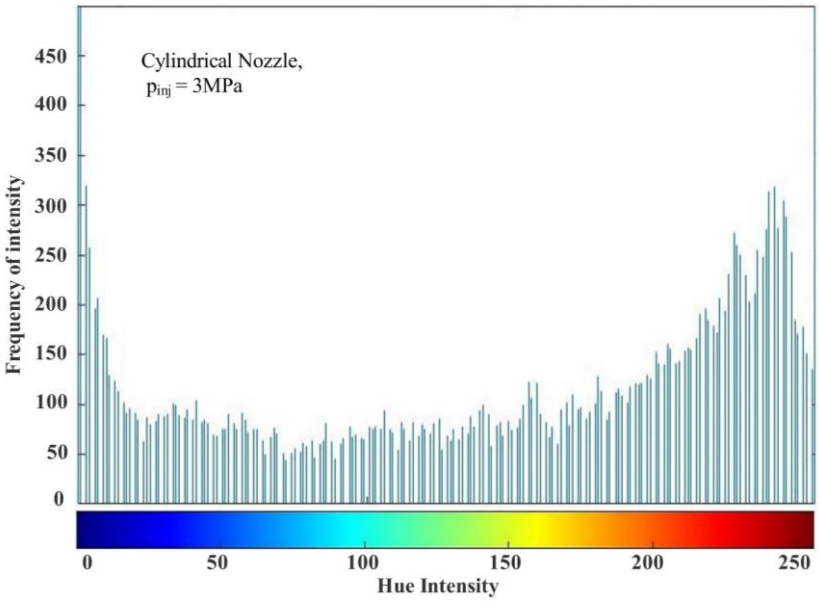

(h)

Fig. 8. The histogram of different nozzle sprays at different injection pressures; a) divergent conical nozzle with p_{inj}=1 MPa, b) cylindrical nozzle with p_{inj}=1 MPa, c) convergent conical nozzle with p_{inj}=1 MPa, d) divergent conical nozzle with p_{inj}=2 MPa, e) cylindrical nozzle with p_{inj}=2 MPa, f) convergent conical nozzle with p_{inj}=2 MPa, g) divergent conical nozzle with p_{inj}=3 MPa, h) cylindrical nozzle with p_{inj}=3 MPa, i) convergent conical nozzle with p_{inj}=3 MPa. (Colntinued)

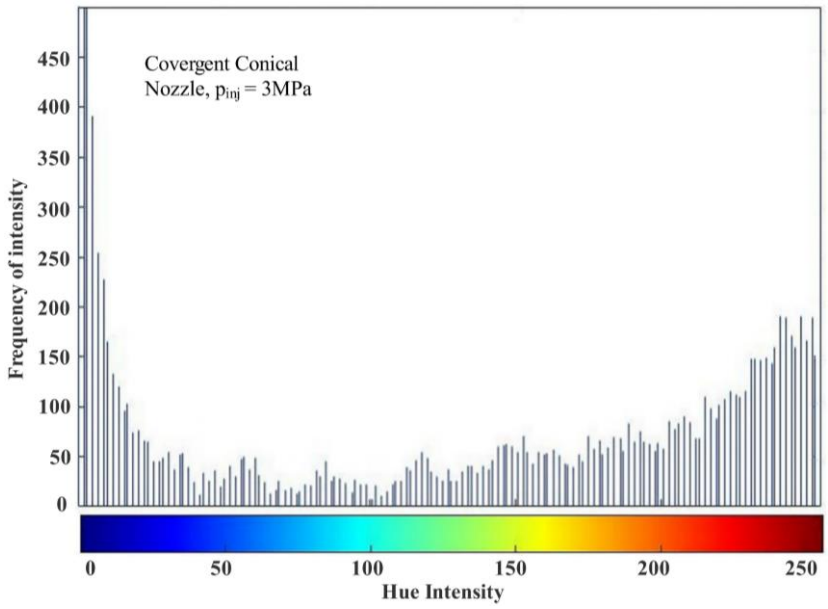

(i)

Fig. 8. The histogram of different nozzle sprays at different injection pressures; a) divergent conical nozzle with p_{inj}=1 MPa, b) cylindrical nozzle with p_{inj}=1 MPa, c) convergent conical nozzle with p_{inj}=1 MPa, d) divergent conical nozzle with p_{inj}=2 MPa, e) cylindrical nozzle with p_{inj}=2 MPa, f) convergent conical nozzle with p_{inj}=2 MPa, g) divergent conical nozzle with p_{inj}=3 MPa, h) cylindrical nozzle with p_{inj}=3 MPa, i) convergent conical nozzle with p_{inj}=3 MPa.

shown on the spray with the increase in spray cone angle by 2 degrees. At an injection pressure of 4 MPa, at which hydraulic flip happens in the nozzle, the spray cone angle was decreased to a little more than half of that at 3 MPa injection pressure (about 19 degrees). Therefore, among this range of injection pressures, it can be concluded that the pressure corresponding to the occurrence of super-cavitation leads to better droplet distribution in the cylindrical nozzle. This fact is also true about the divergent conical nozzle. It can also be inferred that an uncontrolled increase in inlet pressure can cause a non-uniform droplet distribution.

3- 4- Effect of injection pressure on outlet volume flow rate

Fig. 10 compares the volume flow rate of the divergent conical, cylindrical, and convergent conical nozzles at different injection pressures. The results obtained from the experiments show that in the divergent conical nozzle, with the increase of the pressure from 1 to 2 MPa, the volume flow rate increased from 108.9 ml/s to 119.7 ml/s and, with an increase of the pressure up to 3 MPa, the volume flow rate decreased down to 101.3 ml/s. Similarly, for the cylindrical nozzle, the trend was the same; the volume flow rate increased from 116.15 ml/s to 139.6 ml/s with increasing pressure from 1 to 3 MPa and then decreased to 135.1 ml/s with further increasing pressure up to 4 MPa. The increase of the volume flow rate is directly due to the increase of the injection pressure but the decrease of the volume flow rate at a certain pressure, as mentioned in the image process of the spray, is because of happening of the hydraulic flip phenomenon. A comparison of the volume flow rate for all three types of nozzles shows that at a certain pressure, the volume flow rate of the nozzle for the convergent conical nozzle is higher than both the other nozzles. In fact, in a convergent conical nozzle, the frictional losses are lower than the other nozzles; it is because of the greater curvature of the entrance edge of the orifice.

4- Conclusion

In this assignment, the influence of injector nozzle geometry on the internal fluid flow and hydrodynamic behavior of spray was scrutinized. In an experimental study, three transparent injector nozzles including, divergent conical, cylindrical, and convergent conical nozzles, were subjected to different fuel injection pressures. Then, the flow inside the injector nozzle and the spray were recorded using a high-resolution camera. Finally, the results were examined using image processing methods. The examination of fluid

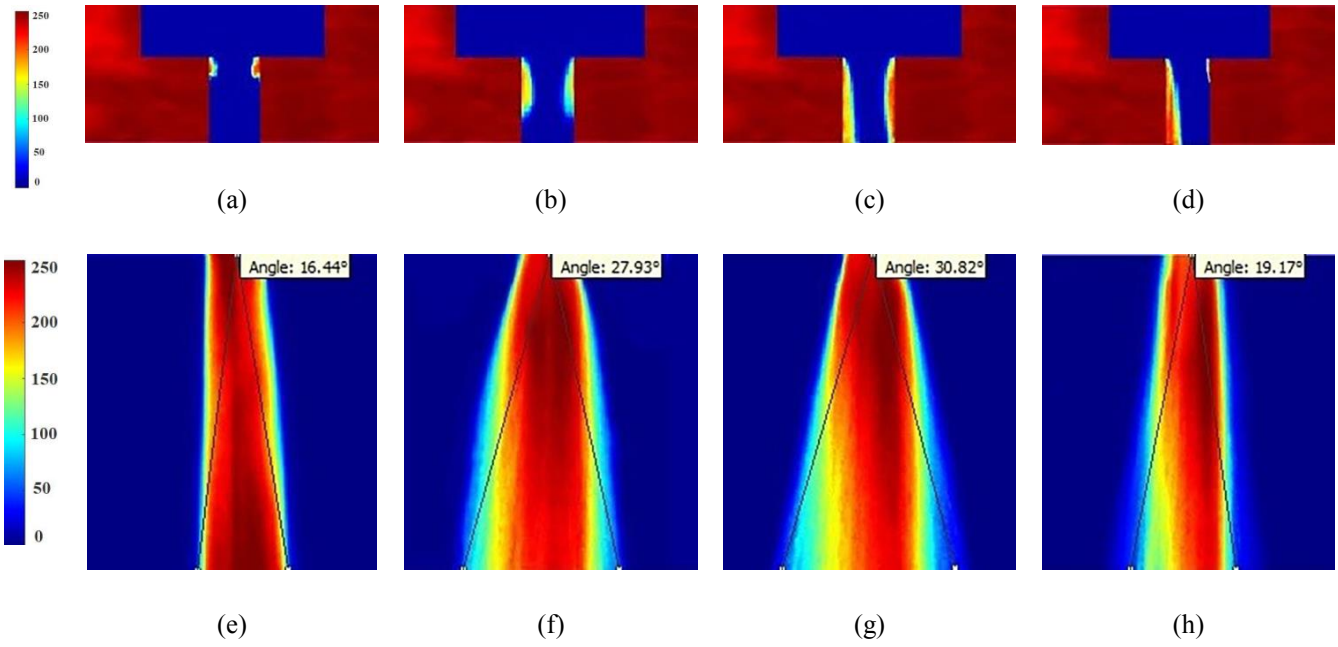

Fig. 9. Flow in cylindrical nozzle and the spray at different injection pressures. (a),(e) p_{inj}=1 MPa, (b),(f) p_{inj}=2 MPa, (c),(g) p_{inj}=3 MPa and (d),(h) p_{inj}=4 MPa

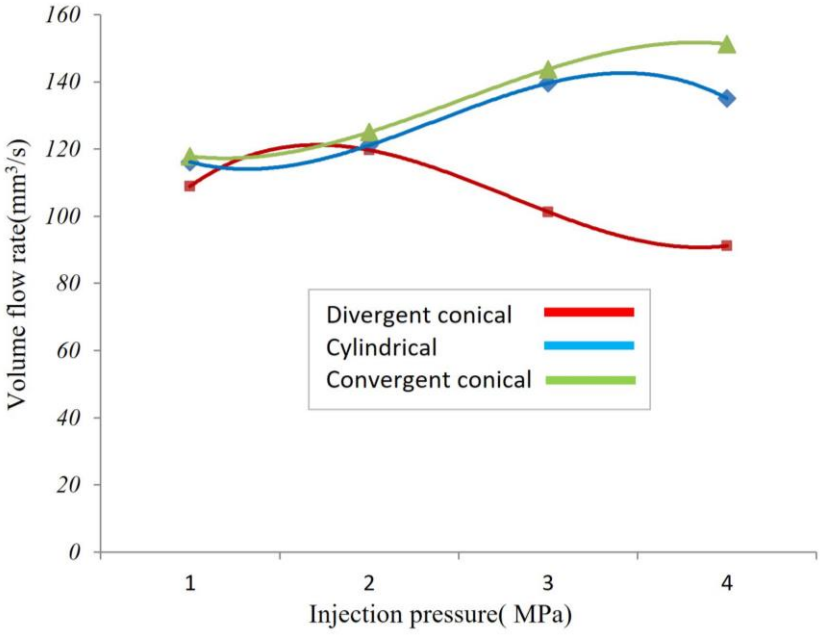

Fig. 10. Volume flow rate of different nozzles

injection pressure's influence on nozzle internal flow revealed that for nozzles with $k \leq 0$, an increase in injection pressure initially leads to an escalation in cavitation bubble formation. However, this phenomenon abruptly diminishes on one side of the nozzle orifice. This occurrence can be attributed to a localized pressure drop to the vapor pressure of the saturated liquid, resulting from a sudden alteration in the inlet cross-section of these nozzle orifices. In divergent conical nozzles, the formation of cavitation bubbles was observed more than in cylindrical nozzles. In this type of nozzle, the inlet curvature of the nozzle orifice is much steeper than the convergent conical and cylindrical nozzles. No cavitation bubbles were seen in the convergent conical nozzle in the used pressure range.

Induced results of the injector nozzle spray showed that the spray cone angle of the divergent conical nozzle is higher than the cylindrical and convergent conical nozzles. This fact is due to two main reasons: firstly, the divergent shape of the nozzle orifice causes the spray exit with a greater diffusion angle, and secondly, the occurrence of cavitation phenomenon with more intensity in this type of nozzle contributes to more turbulence of flow. In general, it can be detected among the three studied nozzles in this survey, that both divergent conical and cylindrical nozzles would have the desired spray in the injection pressure corresponding super-cavitation. Although, the divergent conical nozzle has a wider spray cone angle.

For future endeavors, it would be advantageous to explore various types of nozzles with injection pressures exceeding the current range. Additionally, different types of fluids may yield disparate outcomes, thus warranting further studies.

References

[1] X. Li, H. Zhou, L. Su, Y. Chen, Z. Qiao, F. Liu, Combustion and emission characteristics of a lateral swirl combustion system for DI diesel engines under low excess air ratio conditions, Fuel, 184 (2016) 672-680.

[2] R. Payri, J.P. Viera, V. Gopalakrishnan, P.G. Szymkowicz, The effect of nozzle geometry over internal flow and spray formation for three different fuels, Fuel, 183 (2016) 20-33.

[3] L. Su, X. Li, Z. Zhang, F. Liu, Numerical analysis on the combustion and emission characteristics of forced swirl combustion system for DI diesel engines, Energy conversion and management, 86 (2014) 20-27.

[4] H. Mohammadi, P. Jabbarzadeh, M. Jabbarzadeh, M.T. Shrevani-Tabar, Numerical investigation on the hydrodynamics of the internal flow and spray behavior of diesel fuel in a conical nozzle orifice with the spiral rifling like guides, Fuel, 196 (2017) 419-430.

[5] C. Tang, Z. Feng, C. Zhan, Z. Huang, Experimental study on the effect of injector nozzle K factor on the spray characteristics in a constant volume chamber: Near nozzle spray initiation, the macroscopic and the droplet statistics, Fuel, 202 (2017) 583-594.

[6] Y. Sun, Z. Guan, K. Hooman, Cavitation in diesel fuel injector nozzles and its influence on atomization and spray, Chemical engineering & technology, 42(1) (2019) 6-29.

[7] H. Hiroyasu, Spray breakup mechanism from the hole-type nozzle and its applications, Atomization and sprays, 10(3-5) (2000).

[8] Z. He, H. Zhou, L. Duan, M. Xu, Z. Chen, T. Cao, Effects of nozzle geometries and needle lift on steadier string cavitation and larger spray angle in common rail diesel injector, International Journal of Engine Research, 22(8) (2021) 2673-2688.

[9] B. Biçer, A. Sou, Application of the improved cavitation model to turbulent cavitating flow in fuel injector nozzle, Applied Mathematical Modelling, 40(7-8) (2016) 4712-4726.

[10] Z. He, Y. Chen, X. Leng, Q. Wang, G. Guo, Experimental visualization and LES investigations on cloud cavitation shedding in a rectangular nozzle orifice, International Communications in Heat and Mass Transfer, 76 (2016) 108-116.

[11] F. Salvador, M. Carreres, D. Jaramillo, J. Martínez-López, Comparison of microsac and VCO diesel injector nozzles in terms of internal nozzle flow characteristics, Energy conversion and management, 103 (2015) 284-299.

[12] Q. Li, C. Zong, F. Liu, T. Xue, A. Zhang, X. Song, Numerical and experimental analysis of the cavitation characteristics of orifice plates under high-pressure conditions based on a modified cavitation model, International Journal of Heat and Mass Transfer, 203 (2023) 123782.

[13] J. Cui, H. Lai, J. Li, Y. Ma, Visualization of internal flow and the effect of orifice geometry on the characteristics of spray and flow field in pressure-swirl atomizers, Applied Thermal Engineering, 127 (2017) 812-822.

[14] F.J. Salvador, J.J. López, J. De La Morena, M. Crialesi-Esposito, Experimental investigation of the effect of orifices inclination angle in multihole diesel injector nozzles. Part 1–Hydraulic performance, Fuel, 213 (2018) 207-214.

[15] R. Payri, F.J. Salvador, J. De La Morena, V. Pagano, Experimental investigation of the effect of orifices inclination angle in multihole diesel injector nozzles. Part 2–Spray characteristics, Fuel, 213 (2018) 215-221.

[16] J. Liu, Z. Liu, J. Wu, Z. Li, P. Chen, X. Gu, Visualization experiment and numerical calculation of the cavitation evolution inside the injector ball valve, Fuel, 329 (2022) 125500.

[17] Z.-Y. Sun, G.-X. Li, C. Chen, Y.-S. Yu, G.-X. Gao, Numerical investigation on effects of nozzle's geometric parameters on the flow and the cavitation characteristics within injector's nozzle for a high-pressure common-rail DI diesel engine, Energy Conversion and Management, 89 (2015) 843-861.

[18] Z. Feng, C. Zhan, C. Tang, K. Yang, Z. Huang, Experimental investigation on spray and atomization characteristics of diesel/gasoline/ethanol blends in high pressure common rail injection system, Energy, 112 (2016) 549-561.

[19] L. Guan, C. Tang, K. Yang, J. Mo, Z. Huang, Effect of di-n-butyl ether blending with soybean-biodiesel on spray and atomization characteristics in a common-rail fuel injection system, Fuel, 140 (2015) 116-125.

[20] Y. Dai, X. Zhang, G. Zhang, M. Cai, C. Zhou, Z. Ni, Numerical analysis of influence of cavitation characteristics in nozzle holes of curved diesel engines, Flow Measurement and Instrumentation, 85 (2022) 102172.

[21] M.T. Shervani-Tabar, S. Parsa, M. Ghorbani, Numerical study on the effect of the cavitation phenomenon on the characteristics of fuel spray, Mathematical and Computer Modelling, 56(5-6) (2012) 105-117.

[22] B. Jalili, P. Jalili, Numerical analysis of airflow turbulence intensity effect on liquid jet trajectory and breakup in two-phase cross flow, Alexandria Engineering Journal, 68 (2023) 577-585.

[23] A. Sou, S. Minami, R. Prasetya, R. Pratama, S. Moon, Y. Wada, H. Yokohata, X-ray visualization of cavitation in nozzles with various sizes, ICLASS-15, (2015).

[24] Z. He, Z. Zhang, G. Guo, Q. Wang, X. Leng, S. Sun, Visual experiment of transient cavitating flow characteristics in the real-size diesel injector nozzle, International Communications in Heat and Mass Transfer, 78 (2016) 13-20.

[25] T. Hayashi, M. Suzuki, M. Ikemoto, Visualization of internal flow and spray formation with real size diesel nozzle, in: 12th triennial international conference on liquid atomization and spray systems, ICLASS, 2012, pp. 2-6.

[26] M. Ghiji, L. Goldsworthy, P.A. Brandner, V. Garaniya, P. Hield, Analysis of diesel spray dynamics using a compressible Eulerian/VOF/LES model and microscopic shadowgraphy, Fuel, 188 (2017) 352-366.

[27] Y. Wei, H. Zhang, L. Fan, B. Li, X. Leng, Z. He, Experimental study on influence of pressure fluctuation and cavitation characteristics of nozzle internal flow on near field spray, Fuel, 337 (2023) 126843.

[28] H. Ding, Z. Wang, Y. Li, H. Xu, C. Zuo, Initial dynamic development of fuel spray analyzed by ultra high speed imaging, Fuel, 169 (2016) 99-110.

[29] J.M. Desantes, R. Payri, F.J. Salvador, A. Gil, Development and validation of a theoretical model for diesel spray penetration, Fuel, 85(7-8) (2006) 910-917.

[30] A. Sou, S. Hosokawa, A. Tomiyama, Effects of cavitation in a nozzle on liquid jet atomization, International journal of heat and mass transfer, 50(17-18) (2007) 3575-3582.

HOW TO CITE THIS ARTICLE

S. Azizi, M. T. Shervani-Tabar, Experimental and Image Processing Study on the Effect of the Cavitation Phenomenon in a Nozzle Injector on the Hydrodynamic Behavior of the Spray, AUT J. Mech Eng., 8(1) (2024) 67-82.

DOI: 10.22060/ajme.2024.22847.6080